Turkish Journal of Mathematics

Volume 43 | Number 5 Article 14

1-1-2019

A convergent two-level linear scheme for the generalizedRosenau-KdV-RLW equation

AYHAN AYDIN

Turkish Journal of Mathematics

http://journals.tubitak.gov.tr/math/

Research Article

Turk J Math
(2019) 43: 2226 – 2245

doi:10.3906/mat-1901-110

A convergent two-level linear scheme for the generalized Rosenau–KdV–RLW equation

Ayhan AYDIN*
Department of Mathematics, Faculty of Arts and Sciences, Atılım University, Ankara, Turkey

Received: 18.02.2019 • **Accepted/Published Online:** 18.07.2019 • **Final Version:** 28.09.2019

Abstract: A new convergent two-level finite difference scheme is proposed for the numerical solution of initial value problem of the generalized Rosenau–KdV–RLW equation. The new scheme is second-order, linear, conservative, and unconditionally stable. It contains one free parameter. The impact of the parameter to error of the numerical solution is studied. The prior estimate of the finite difference solution is obtained. The existence, uniqueness, and convergence of the scheme are proved by the discrete energy method. Accuracy and reliability of the scheme are tested by simulating the solitary wave graph of the equation. Wave generation subject to initial Gaussian condition has been studied numerically. Different wave generations are observed depending on the dispersion coefficients and the nonlinear advection term. Numerical experiments indicate that the present scheme is conservative, efficient, and of high accuracy, and well simulates the solitary waves for a long time.

Key words: Rosenau–KdV–RLW equation, conservative finite difference scheme, convergence, a priori error estimate

1. Introduction

Partial differential equations (PDEs) arise frequently as a mathematical model of fundamental laws of nature. Many problems in applied mathematics, mathematical physics, engineering, and health science are described by a PDE with the appropriate initial and/or boundary conditions.

In the last several decades, many mathematical models have been proposed to understand the theory of wave motion such as the well-known Korteweg-de Vries (KdV) equation [6, 13]

$$u_t + u_{xxx} + 3\left(u^2\right)_x = 0, \qquad 0 \le x \le L,\ 0 \le t \le T. \tag{1.1}$$

Recently, a direct rational exponential scheme is offered to construct exact multisoliton solutions of the nonlinear Calogero–Bogoyavlenskii–Schiff equation and the KdV equation [33]. A numerical technique based on the finite difference and collocation methods is presented for the solution of the KdV equation [15]. In [20], a new exact solitary wave solutions of the extended KdV equation is obtained. In [18], the (G'/G) expansion method was used to construct periodic wave and solitary wave solutions of some nonlinear evolution equations. Rosenau [31, 32] noticed that this model cannot be enough to understand wave–wave or wave–wall interaction, since it has a number of shortcomings as it describes a unidirectional propagation of waves. Moreover, since the KdV equation (1.1) was derived under the assumption of weak anharmonicity, both the shape and the behavior of

*Correspondence: ayhan.aydin@atilim.edu.tr
2010 *AMS Mathematics Subject Classification:*65M06, 65N12 , 35Q53

high-amplitude waves cannot be described by this equation. To overcome these difficulties, Rosenau suggested the so-called Rosenau equation:

$$u_t + u_x + u_{xxxxt} + \frac{1}{2}\left(u^2\right)_x = 0, \qquad 0 \le x \le L,\ 0 \le t \le T. \tag{1.2}$$

Since then, various works have been done for further consideration of nonlinear dispersive waves. To describe the small-amplitude long wave of water in a channel, the so-called regularized long-wave (RLW) equation (also known as the Benjamin–Bona–Mahony equation)

$$u_t + u_x - u_{xxt} + \frac{1}{2}\left(u^2\right)_x = 0, \qquad 0 \le x \le L,\ 0 \le t \le T. \tag{1.3}$$

is proposed [26]. There are lots of numerical studies on this equation such as the finite element method [12], Petrov–Galerkin method [8], local discontinuous Galerkin (LDG) method [38], finite difference method [1], and He's variation iteration method [14] and a perturbation iteration method [4]. In [5], the authors applied the new optimal perturbation iteration method to solve the generalized RLW equation.

In addition to the Rosenau equation (1.2), for further consideration of the nonlinear wave, the viscous term u_{xxx} is included in (1.2)

$$u_t + u_x + u_{xxx} + u_{xxxxt} + \frac{1}{2}\left(u^2\right)_x = 0, \qquad 0 \le x \le L,\ 0 \le t \le T. \tag{1.4}$$

This equation is called the Rosenau–KdV equation. Many analytical and numerical studies have been developed for the Rosenau–KdV equation such as the solitary wave solution and periodic solutions [41], tanh method and sine–cosine method, the tanh-coth method, and first integral method [7]. A conservative finite difference scheme for the solution of the equation (1.4) is developed in [11]. The equation in (1.4) was further extended into the generalized Rosenau–KdV equation

$$u_t + u_x + u_{xxx} + u_{xxxxt} + \left(u^p\right)_x = 0, \qquad 0 \le x \le L,\ 0 \le t \le T, \tag{1.5}$$

where $p \ge 2$ is an integer. In [9, 28], authors discussed the solitary wave solution of the generalized Rosenau-KdV equation. Saha [34] discussed the topological soliton solution or the shock solution of this equation. A conservative Crank–Nicolson finite difference scheme for an initial-boundary value problem of the generalized Rosenau–Kdv equation is proposed in [16].

The generalization of the Rosenau equation (1.2) combined with the RLW equation (1.3) is usually called the Rosenau–RLW (RRLW) equation:

$$u_t + u_x - u_{xxt} + u_{xxxxt} + \frac{1}{2}\left(u^2\right)_x = 0, \qquad 0 \le x \le L,\ 0 \le t \le T. \tag{1.6}$$

In [21, 24, 42], authors proposed a conservative finite difference scheme for the the equation (1.6). In [2], Galerkin finite element method is used for the numerical solution of RRLW equation (1.6). The further extension of the equation (1.6) is the generalized Rosenau–RLW equation:

$$u_t + u_x - u_{xxt} + u_{xxxxt} + \left(u^p\right)_x = 0, \qquad 0 \le x \le L,\ 0 \le t \le T, \tag{1.7}$$

where $p \geq 2$ is an integer. Various numerical methods have been proposed for the numerical solution of the generalized Rosenau–RLW equation. It is solved numerically by the Crank–Nicolson scheme in [42]. Some conservative three-level linearly implicit finite difference schemes for $p \geq 2$ are proposed in [22, 23]. In [19], the equation is solved by using the quintic B-splines collocation method. In [17], the SRLW equation is studied via a new analytical approach.

The Rosenau–Korteweg de Vries equation (1.5) coupled with the general Rosenau-Regularized Long Wave equation (1.7)

$$u_t + u_x + \beta u_{xxx} - \gamma u_{xxt} + u_{xxxxt} + \alpha(u^p)_x = 0 \tag{1.8}$$

is proposed as another model to study the shallow water waves [29] and known as the Rosenau–KdV–RLW equation with power law nonlinearity or generalized Rosenau–KdV–RLW equation. Although there have been a lot of previous works on the numerical solutions of the equations (1.1)–(1.7), little attention has been given to the analytical and the numerical solution of the generalized Rosenau–KdV–RLW equation (1.8). Razborova et al. [30] applied soliton perturbation theory to obtain the adiabatic dynamics of soliton parameters. Also analytical one soliton solution of the perturbed Rosenau–KdV–RLW equation is obtained. As far as computational studies are concerned, Wongsaijai and Poochinapan [37] proposed a conservative three-level average implicit finite difference method and Wang and Dai [36] proposed a three-level linear implicit conservative scheme to solve the equation (1.8). However, three-level schemes suffer from the initial condition. When the initial condition u_j^0 is given, three-level scheme in [36, 37] cannot start the iteration. Another two-level conservative scheme is required to compute u_j^1 for the proposed scheme in [36, 37]. Pan et al. proposed a new Crank–Nicolson pseudo compact conservative finite difference scheme [25]. The proposed scheme in [25] is two-level but nonlinear, it numerically simulates the conservative laws at the same time. Nevertheless nonlinear schemes require an iterative method such as the Newton method which has high cost per time step. To our knowledge, there is no two-level and linear conservative scheme for the numerical solution of the generalized Rosenau–KdV–RLW equation (1.8). The aim of this paper is to propose a method which is two-level and linear for the numerical solution of the generalized Rosenau–KdV–RLW equation (1.8). The proposed scheme is second-order, unconditionally stable and conservative. In addition, although the proposed methods in [25] and [37] are energy conserving only for $p = 2$, the present scheme in this paper is energy conserving for all $p \geq 2$.

The remainder of this paper is organized as follows: In Section 2 a two-level, linear, energy conserving scheme is proposed for the generalized Rosenau–KdV–RLW equation (1.8). In Section 3, the prior estimates, existence, uniqueness, stability, and second-order convergence of the numerical solution are proved. Section 4 is devoted to numerical results to verify the reliability and the efficiency of the proposed scheme. Finally, a conclusion is given in Section 5.

2. A conservative finite difference scheme

In this section we will consider the generalized Rosenau–KdV–RLW equation

$$u_t + u_x + \beta u_{xxx} - \gamma u_{xxt} + u_{xxxxt} + \alpha(u^p)_x = 0 \tag{2.1}$$

in the domain $(x,t) \in [x_L, x_R] \times [0,T]$ with the initial condition

$$u(x,0) = u_0(x), \quad x_L \leq x \leq x_R \tag{2.2}$$

and the boundary conditions

$$u(x_L,t)=u_x(x_L,t)=0,\quad u(x_R,t)=u_x(x_R,t)=0. \tag{2.3}$$

The assumption that $u\to 0$ as $x\to x_L$ and $x\to x_R$ imply two conservation laws, namely the mass conservation

$$Q(t)=\int_{x_L}^{x_R} u(x,t)\,dx=Q(0) \tag{2.4}$$

and the energy conservation

$$\begin{aligned} E(t) &= \int_{x_L}^{x_R}\left[u^2(x,t)+\gamma u_x^2(x,t)+u_{xx}^2(x,t)\right]\,dx \\ &= \|u\|_{L_2}^2+\gamma\|u_x\|_{L_2}^2+\|u_{xx}\|_{L_2}^2=E(0). \end{aligned} \tag{2.5}$$

For the numerical solution of the initial-boundary value problem (2.1)–(2.3), we introduce the equally distributed grid points $x_j=x_L+jh,\ j=0,1,\cdots,J$, and $t_n=n\tau,\ n=1,2,\cdots,N+1$, where J and N are integers, $h=(x_R-x_L)/J$ and $\tau=T/N$ are the spatial and temporal step sizes, respectively. Let u_j^n be the approximation to the exact solution $u(x,t)$ at the mesh point (x_j,t_n) and $Z_h^0=\{u=(u_j)|u_{-1}=u_0=u_J=u_{J+1}=0,\ j=-1,0,1,\cdots,J,J+1\}$. We use the following notation for the difference operators, inner product and norm:

$$\begin{aligned} &\left(u_j^n\right)_x=\frac{u_{j+1}^n-u_j^n}{h}, && \left(u_j^n\right)_{\overline{x}}=\frac{u_j^n-u_{j-1}^n}{h}, && \left(u_j^n\right)_{\hat{x}}=\frac{u_{j+1}^n-u_{j-1}^n}{2h} \\ &\left(u_j^n\right)_t=\frac{u_j^{n+1}-u_j^n}{\tau}, && \left(u_j^n\right)_{x\overline{x}}=\frac{u_{j+1}^n-2u_j^n+u_{j-1}^n}{h^2}, && \left(u_j^{n+1/2}\right)=\frac{u_j^{n+1}+u_j^n}{2} \\ &<u^n,v^n>=h\sum_{j=1}^{J-1}u_j^nv_j^n, && \|u^n\|^2=<u^n,u^n>, && \|u^n\|_\infty=\max_{0\le j\le J-1}|u_j^n|. \end{aligned}$$

The following two-level linear finite difference scheme is proposed for the numerical solution of the initial-boundary value problem (2.1)–(2.3)

$$\left(u_j^n\right)_t+\left(u_j^{n+1/2}\right)_{\hat{x}}+\beta\left(u_j^{n+1/2}\right)_{x\overline{x}\hat{x}}-\gamma\left(u_j^n\right)_{x\overline{x}t}+\left(u_j^n\right)_{xx\overline{x}\,\overline{x}\,t}+\alpha\kappa\left(u_j^n,u_j^{n+1/2}\right)=0, \tag{2.6}$$

where

$$\kappa\left(u_j^n,u_j^{n+1/2}\right)=p\theta\left(u_j^n\right)^{p-1}\left(u_j^{n+1/2}\right)_{\hat{x}}+(1-\theta)\left[\left(u_j^n\right)^{p-1}u_j^{n+1/2}\right]_{\hat{x}},\quad \theta\in\mathbb{R} \tag{2.7}$$

$$u_0^n=u_J^n=0,\quad j=1,2,\cdots,J-1 \tag{2.8}$$

$$\left(u_0^n\right)_{\hat{x}}=\left(u_J^n\right)_{\hat{x}}=0,\left(u_0^n\right)_{x\overline{x}}=\left(u_J^n\right)_{x\overline{x}}=0,u_j^0=u_0(x_j). \tag{2.9}$$

To analyze the discrete conservation laws of the proposed two-level linear scheme (2.6), we introduce the following lemma.

Lemma 2.1 *[40] For any two mesh functions $u, v \in Z_h^0$, we have*

$$< u_x, v >= - < u, v_{\overline{x}} >, \quad < u_{\hat{x}}, v >= - < u, v_{\hat{x}} >, \quad < u, v_{x\overline{x}} >= - < u_x, v_x > . \tag{2.10}$$

Then we have

$$< u, u_{x\overline{x}} >= - < u_x, u_x >= -\|u_x\|^2. \tag{2.11}$$

Furthermore, if $(u_0^n)_{x\overline{x}} = (u_J^n)_{x\overline{x}} = 0$, then

$$< u, u_{xx\overline{x}\overline{x}} >= \|u_{x\overline{x}}\|^2$$

Theorem 2.2 *Suppose $u_0 \in H_0^2[x_L, x_R]$ and $p = 2$. If the nonlinear term $(u^p)_x$ in (2.1) is discretized as*

$$p\theta \left(u_j^n\right)^{p-1} \left(\overline{u}_j^n\right)_{\hat{x}} + (1-\theta) \left[\left(u_j^n\right)^{p-1} \overline{u}_j^n\right]_{\hat{x}},$$

then the scheme (2.6) is mass conserving in the sense:

$$Q^n = h \sum_{h=1}^{J-1} \left(u_j^n + \tau\theta u_j^{n-1} (u_j^n)_{\hat{x}}\right) = Q^{n-1} = \cdots = Q^0, \tag{2.12}$$

where $\overline{u}_j^n = (u_j^{n+1} - u_j^{n-1})/(2\tau)$.

Proof Multiplying Eq. (2.6) by τh, summing up from $j = 1$ to $j = J-1$, and using the Lemma 1, it follows that

$$h \sum_{j=1}^{J-1} \left(u_j^{n+1} + \tau\theta u_j^n (u_j^{n+1})_{\hat{x}}\right) = h \sum_{j=1}^{J-1} \left(u_j^n + \tau\theta u_j^{n-1} (u_j^n)_{\hat{x}}\right). \tag{2.13}$$

If we set

$$Q^n = h \sum_{h=1}^{J-1} \left(u_j^n + \tau\theta u_j^{n-1} (u_j^n)_{\hat{x}}\right),$$

we obtain Eq. (2.12). □

Theorem 2.3 *Suppose $u_0 \in H_0^2[x_L, x_R]$ and $\theta = \frac{1}{p+1}$, then the scheme (2.6) admits the discrete energy*

$$E(t_n) = \|\mathbf{u}^n\|^2 + \gamma\|\mathbf{u}_x^n\|^2 + \|\mathbf{u}_{x\overline{x}}^n\|^2 = E^{n-1} = \cdots = E(t_0). \tag{2.14}$$

Proof Computing the inner product of (2.6) with $2u_j^{n+1/2}$ (i.e. $u_j^{n+1} + u_j^n$), we have

$$\begin{aligned} \left(u_j^n\right)_t \cdot 2u_j^{n+1/2} + & \left(u_j^{n+1/2}\right)_{\hat{x}} \cdot 2u_j^{n+1/2} + \beta \left(u_j^{n+1/2}\right)_{x\overline{x}\hat{x}} \cdot 2u_j^{n+1/2} \\ & -\gamma \left(u_j^n\right)_{x\overline{x}t} \cdot 2u_j^{n+1/2} + \left(u_j^n\right)_{xx\overline{x}\,\overline{x}\,t} \cdot 2u_j^{n+1/2} \\ & +\alpha\kappa \left(u_j^n, u_j^{n+1/2}\right) \cdot 2u_j^{n+1/2} = 0, \end{aligned} \tag{2.15}$$

where $\kappa\left(u_j^n, u_j^{n+1/2}\right)$ is defined in (2.7). The first term of (2.15) is written as

$$h\sum_{j=1}^{J-1}(u_j^n)_t(u_j^{n+1}+u_j^n)=\frac{1}{\tau}\left(\|u^{n+1}\|^2-\|u^n\|^2\right). \tag{2.16}$$

Using homogeneous boundary conditions, the second term of (2.15) is written as

$$h\sum_{j=1}^{J-1}\left(u_j^{n+1/2}\right)_{\hat{x}}2u_j^{n+1/2}=0. \tag{2.17}$$

According to

$$< u_{x\bar{x}\hat{x}},u >=< u_{x\bar{x}},u_{\hat{x}} >=< u_x,u_{x\hat{x}} >=-< u,u_{x\bar{x}\hat{x}} >$$

the third term is reduced to

$$\beta h\sum_{j=1}^{J-1}\left(u_j^{n+1/2}\right)_{x\bar{x}\hat{x}}\cdot 2u_j^{n+1/2}=0. \tag{2.18}$$

From Lemma 2.1, the fourth term of (2.15) is written as

$$\gamma h\sum_{j=1}^{J-1}\left(u_j^n\right)_{x\bar{x}t}2u_j^{n+1/2}=\frac{\gamma}{\tau}\left(-\|u_x^{n+1}\|^2+\|u_x^n\|^2\right). \tag{2.19}$$

Similarly, the fifth term is written as

$$h\sum_{j=1}^{J-1}\left(u_j^n\right)_{xx\bar{x}\,\bar{x}\,t}2u_j^{n+1/2}=\frac{1}{\tau}\left(\|u_{x\bar{x}}^{n+1}\|^2-\|u_{x\bar{x}}^n\|^2\right). \tag{2.20}$$

Using the discrete boundary conditions (2.9) and Lemma 2.1, after tedious calculation it can be shown that

$$\alpha h\sum_{j=1}^{J-1}\kappa\left(u_j^n,u_j^{n+1/2}\right)2u_j^{n+1/2}=0. \tag{2.21}$$

From (2.16)–(2.20), we get (2.14). This completes the proof. □

Remark 2.4 *The existence of the above discrete conservation laws is essential for the stability and convergence of the scheme (2.6). The discrete energy conservation (2.14) confirms that the energy would not increase in time; therefore, the scheme (2.6)–(2.9) will never show numerical blow-up.*

3. Numerical analysis of the scheme

In this section, existence of the solution, the unique solvability, convergence and stability of the difference solution for (2.6)–(2.9) are proved.

3.1. A priori estimation

In this section, we shall make some prior estimations for the difference scheme (2.6). We need the following lemma.

Lemma 3.1 *(Discrete Sobolev's inequality [40]). There exists two constants c_1 and c_2 such that*

$$\|u^n\|_\infty \leq c_1\|u^n\| + c_2\|u_x^n\| \tag{3.1}$$

Theorem 3.2 *Suppose $u_0 \in H_0^2[x_L, x_R]$, then the following inequalities*

$$\|u^n\| \leq C, \quad \|u_{xx}^n\| \leq C, \quad \|u^n\|_\infty \leq C, \tag{3.2}$$

for $n = 1, 2, \cdots, N$, hold for the solution u^n of (2.6)–(2.9).

Proof If $\gamma > 0$, then it follows from (2.14) that

$$\|u^n\| \leq C, \quad \|u_{x\bar{x}}^n\| \leq C$$

for any $0 \leq n \leq N$. By using Lemma 1, and the Cauchy–Schwartz inequality, we have

$$\|u_x^n\| = - < u^n, u_{x\bar{x}}^n > \leq \|u^n\|\|u_{x\bar{x}}^n\| \leq \frac{1}{2}\left(\|u^n\|^2 + \|u_{x\bar{x}}^n\|^2\right) \leq C.$$

From Lemma 4, we have $\|u^n\|_\infty \leq C$.

If $\gamma \leq 0$, then from (2.14) we have

$$\|\mathbf{u}^n\|^2 + \gamma\|\mathbf{u}_x^n\|^2 + \|\mathbf{u}_{x\bar{x}}^n\|^2 \leq \|\mathbf{u}^n\|^2 + \frac{\gamma}{2}\left(\|u^n\|^2 + \|\mathbf{u}_{x\bar{x}}^n\|^2\right) + \|\mathbf{u}_{x\bar{x}}^n\|^2$$

$$= \left(1 + \frac{\gamma}{2}\right)\|u^n\|^2 + \left(1 + \frac{\gamma}{2}\right)\|u_{x\bar{x}}^n\|^2 \leq C$$

under the condition that $1 + \frac{\gamma}{2} > 0$. This completes the proof. □

Remark 3.3 *Theorem 3.2 implies that the scheme (2.6)–(2.9) is unconditionally stable.*

3.2. Existence and uniqueness

In this section, we will prove the existence and uniqueness of the numerical solution of the initial-boundary value problem (2.6)–(2.9).

Theorem 3.4 *The solution of the difference scheme (2.6)–(2.9) exists and is unique.*

Proof It is clear that u^{n+1} can be solved from (2.6) since the scheme (2.6) is linear, which guaranties the existence of solution. It is obvious that u^0 is determined from the initial condition (2.8). By mathematical induction, suppose that $u^1, u^2, \cdots, u^n, (n = 1, 2, \cdots, N-1)$ are solved uniquely. Consider the method (2.6) for u^{n+1}. Assume $u^{n+1,1}$ and $u^{n+1,2}$ are two solutions of (2.6). Let us define

$$W^{n+1} = u^{n+1,1} - u^{n+1,2}. \tag{3.3}$$

Then it is easy to verify that W^{n+1} satisfies the equation

$$\frac{1}{\tau}W_j^{n+1}+\frac{1}{2}\left(W_j^{n+1}\right)_{\hat{x}}-\frac{1}{\tau}\gamma\left(W_j^{n+1}\right)_{x\overline{x}}+\frac{1}{\tau}\left(W_j^{n+1}\right)_{xx\overline{x}\,\overline{x}}+\frac{1}{2}\alpha\kappa\left(u_j^n,W_j^{n+1}\right)=0, \tag{3.4}$$

where

$$\kappa\left(u_j^n,W_j^{n+1}\right)=p\theta\left(u_j^n\right)^{p-1}\left(W_j^{n+1}\right)_{\hat{x}}+(1-\theta)\left[\left(u_j^n\right)^{p-1}W_j^{n+1}\right]_{\hat{x}} \tag{3.5}$$

Taking the inner product of (3.4) by W_j^{n+1}, we have

$$\|W^{n+1}\|^2+\gamma\|W_x^{n+1}\|^2+\|W_{x\overline{x}}^{n+1}\|^2=0. \tag{3.6}$$

By the definition of norm, it follows that there is a trivial solution $W_j^{n+1}=0$. From the definition (3.3) we have

$$u^{n+1,1}=u^{n+1,2}.$$

Therefore, U^{n+1} is determined uniquely from the scheme (2.6). This completes the proof. □

3.3. Convergence and stability

Let $v_j^n=v(x_j,t_n)$ be the analytical solution of the scheme, then the local truncation error is

$$\begin{aligned}R_j^n &= (v_j^n)_t-\gamma^{RLW}(v_j^n)_{x\overline{x}t}+(v_j^n)_{xx\overline{x}\overline{x}t}+\beta(v_j^{n+1/2})_{x\overline{x}\hat{x}}+(v_j^{n+1/2})_{\hat{x}}\\ &\quad+\alpha p\theta(v_j^n)^{p-1}(v_j^{n+1/2})_{\hat{x}}+\alpha(1-\theta)\left[(v_j^n)^{p-1}v_j^{n+1/2}\right]_{\hat{x}}.\end{aligned} \tag{3.7}$$

By using Taylor expansion it is easy to show that $R_j^n=\mathcal{O}(h^2+\tau^2)$ holds as $h\to 0$ and $\tau\to 0$.

Lemma 3.5 *(Discrete Gronwall inequality [40]). Suppose $\omega(k)$ and $\rho(k)$ are nonnegative functions and $\rho(k)$ is nondecreasing. If $C>0$, and*

$$\omega(k)\le\rho(k)+C\tau\sum_{l=0}^{k-1}\omega(k),\quad\forall k$$

then

$$\omega(k)\le\rho(k)\,\exp(C\tau uk),\quad\forall k.$$

Theorem 3.6 *Let $u_0\in H_0^2[x_L,x_R]$ then the solution u^n of the difference scheme (2.6)–(2.9) converges to the solution $v(x,t)$ of problem (2.1)–(2.3) in with the rate of convergence $\mathcal{O}(h^2+\tau^2)$ by the norm $\|\cdot\|_\infty$.*

Proof Subtracting (2.6) from (3.7) and defining the error $e_j^n=v(x_j,t_n)-u_j^n$ at the mesh point (x_j,t_n), we get

$$\begin{aligned}R_j^n &= (e_j^n)_t-\gamma^{RLW}(e_j^n)_{x\overline{x}t}+(e_j^n)_{xx\overline{x}\overline{x}t}+\beta(e_j^{n+1/2})_{x\overline{x}\hat{x}}+(e_j^{n+1/2})_{\hat{x}}\\ &\quad+\alpha p\theta(u_j^n)^{p-1}(u_j^{n+1/2})_{\hat{x}}+\alpha(1-\theta)\left[(u_j^n)^{p-1}u_j^{n+1/2}\right]_{\hat{x}}\\ &\quad-\alpha p\theta(v_j^n)^{p-1}(v_j^{n+1/2})_{\hat{x}}-\alpha(1-\theta)\left[(v_j^n)^{p-1}v_j^{n+1/2}\right]_{\hat{x}}.\end{aligned} \tag{3.8}$$

Computing the inner product of (3.8) with $2e^{n+1/2}$, we have

$$h\sum_{j=1}^{J-1}\left\{\left(\frac{e_j^{n+1}-e_j^n}{\tau}\right)\right. \quad \cdot 2e^{n+1/2}-\gamma^{RLW}(e_j^n)_{x\overline{x}t}\cdot 2e^{n+1/2}+(e_j^n)_{xx\overline{x}\overline{x}t}\cdot 2e^{n+1/2}$$
$$+\beta(e_j^{n+1/2})_{x\overline{x}\hat{x}}\cdot 2e^{n+1/2}+(e_j^{n+1/2})_{\hat{x}}\cdot 2e^{n+1/2}$$
$$\left.-P\cdot 2e^{n+1/2}-Q\cdot 2e^{n+1/2}\right\}$$

where

$$\begin{aligned} P &= \alpha p\theta(v_j^n)^{p-1}(v_j^{n+1/2})_{\hat{x}}-\alpha p\theta(u_j^n)^{p-1}(u_j^{n+1/2})_{\hat{x}} \\ Q &= \alpha(1-\theta)\left[(v_j^n)^{p-1}v_j^{n+1/2}\right]_{\hat{x}}-\alpha(1-\theta)\left[(u_j^n)^{p-1}u_j^{n+1/2}\right]_{\hat{x}}. \end{aligned} \tag{3.9}$$

The first term of (3.9) gives

$$\frac{1}{\tau}\left(\|e^{n+1}\|^2-\|e^n\|^2\right). \tag{3.10}$$

According to Lemma 1 and the definitions of $(e_j^n)_{x\overline{x}t}$ and $(e_j^n)_{xx\overline{x}\overline{x}t}$, we have

$$\begin{aligned} (e_j^n)_{x\overline{x}t}\cdot 2e^{n+1/2} &= -\frac{1}{\tau}\left(\|e_x^{n+1}\|^2-\|e_x^n\|^2\right), \\ (e_j^n)_{xx\overline{x}\overline{x}t}\cdot 2e^{n+1/2} &= \frac{1}{\tau}\left(\|e_{x\overline{x}}^{n+1}\|^2-\|e_{x\overline{x}}^n\|^2\right), \end{aligned} \tag{3.11}$$

Similarly, it follows from the fourth and fifth terms of (3.9) that

$$\begin{aligned} (e_j^{n+1/2})_{x\overline{x}\hat{x}}\cdot 2e^{n+1/2} &= 0, \\ (e_j^{n+1/2})_{\hat{x}}\cdot 2e^{n+1/2} &= 0. \end{aligned} \tag{3.12}$$

According to Lemma 1 and the Cauchy–Schwartz inequality, we get

$$\begin{aligned} P\cdot 2e^{n+1/2} &= \alpha p\theta\left\{(v_j^n)^{p-1}(v_j^{n+1/2})_{\hat{x}}-(u_j^n)^{p-1}(u_j^{n+1/2})_{\hat{x}}\right\}\cdot 2e^{n+1/2} \\ &= \alpha p\theta 2h\sum_{j=1}^{J-1}\left[(v_j^n)^{p-1}\left\{(e_j^{n+1/2})_{\hat{x}}+(u_j^{n+1/2})_{\hat{x}}\right\}-(u_j^n)^{p-1}(u_j^{n+1/2})_{\hat{x}}\right]\ e^{n+1/2} \\ &= \alpha p\theta 2h\sum_{j=1}^{J-1}\left[(v_j^n)^{p-1}(e_j^{n+1/2})_{\hat{x}}e_j^{n+1/2}+\left\{(v_j^n)^{p-1}-(u_j^n)^{p-1}\right\}u_j^{n+1/2}e_j^{n+1/2}\right] \\ &= \alpha p\theta 2h\sum_{j=1}^{J-1}\left((v_j^n)^{p-1}(e_j^{n+1/2})_{\hat{x}}e_j^{n+1/2}+e_j^n\left\{\sum_{k=0}^{p-2}(v_j^n)^{p-2-k}(u_j^n)^k\right\}u_j^{n+1/2}e_j^{n+1/2}\right) \\ &\le Ch\sum_{j=1}^{J-1}\left[\left|(e_j^{n+1/2})_{\hat{x}}\right|+\left|e_j^n\right|\right]e_j^{n+1/2} \\ &\le Ch\left[\|e_x^{n+1}\|^2+\|e_x^n\|^2+\|e^{n+1}\|^2+\|e^n\|^2\right] \end{aligned} \tag{3.13}$$

and

$$\begin{aligned} P\cdot 2e^{n+1/2} &= \alpha(1-\theta)2h\sum_{j=1}^{J-1}\left\{-(v_j^n)^{p-1}v_j^{n+1/2}+(u_j^n)^{p-1}u_j^{n+1/2}\right\}(e_j^{n+1/2})_{\hat{x}} \\ &= -\alpha(1-\theta)2h\sum_{j=1}^{J-1}\left\{(v_j^n)^{p-1}\left(e_j^{n+1/2}+u_j^{n+1/2}\right)-(u_j^n)^{p-1}u_j^{n+1/2}\right\}(e_j^{n+1/2})_{\hat{x}} \\ &= -\alpha(1-\theta)2h\sum_{j=1}^{J-1}\left\{\left((v_j^n)^{p-1}-(u_j^n)^{p-1}\right)u_j^{n+1/2}+v_j^{n+1/2}e_j^{n+1/2}\right\}(e_j^{n+1/2})_{\hat{x}} \\ &= -\alpha(1-\theta)2h\sum_{j=1}^{J-1}\left\{e_j^n\left(\sum_{k=0}^{p-2}(v_j^n)^{p-2-k}(u_j^n)^k\right)u_j^{n+1/2}+v_j^{n+1/2}e_j^{n+1/2}\right\}(e_j^{n+1/2})_{\hat{x}} \\ &\le Ch\sum_{j=1}^{J-1}\left[\left|(e_j^n)\right|+\left|e_j^{n+1/2}\right|\right]e_j^{n+1/2} \\ &\le Ch\left[\|e^{n+1}\|^2+\|e^n\|^2+\|e_x^{n+1}\|^2+\|e_x^n\|^2\right]. \end{aligned} \tag{3.14}$$

Moreover,

$$\begin{aligned} R_j^n\cdot 2e^{n+1/2} &\le h\sum_{j=1}^{J-1}(R_j^n)^2+\frac{h}{2}\sum_{j=1}^{J-1}\left\{(e_j^{n+1})^2+(e_j^n)^2\right\} \\ &= \|R^n\|^2+\frac{1}{2}\left(\|e^{n+1}\|^2+\|e^n\|^2\right) \\ &\le \|R^n\|^2+\|e^{n+1}\|^2+\|e^n\|^2 \end{aligned} \tag{3.15}$$

Substituting (3.9)–(3.15) into (3.8), it can be shown that

$$\begin{aligned} \|e^{n+1}\|^2- \quad &\|e^n\|^2+\gamma^{RLW}\left(\|e_x^{n+1}\|^2-\|e_x^n\|^2\right)+\left(\|e_{xx}^{n+1}\|^2-\|e_{xx}^n\|^2\right)\le\tau\|R^n\|^2 \\ &+C\tau h\left[\|e_x^{n+1}\|^2+\|e_x^n\|^2+\|e^{n+1}\|^2+\|e^n\|^2+\|e_{xx}^{n+1}\|^2+\|e_{xx}^n\|^2\right] \end{aligned} \tag{3.16}$$

where we have used

$$\|e_x^n\|\le\frac{1}{2}\left(\|e^n\|^2+\|e_{xx}^n\|^2\right) \tag{3.17}$$

Let $D=\|e^n\|^2+\gamma^{RLW}\|e_x^n\|^2+\|e_{xx}^n\|^2$, then (3.16) can be written as

$$(1-C\tau)(D^{n+1}-D^n)\le\tau\|R^n\|^2+2C\tau D^n \tag{3.18}$$

When τ is sufficiently small satisfying $1-C\tau>0$, then

$$D^{n+1}-D^n\le C\tau\|R^n\|^2+C\tau D^n \tag{3.19}$$

Summing up (3.19) from 0 to $n-1$, we have

$$D^n\le D^0+C\tau\sum_{k=0}^{n-1}\|R^k\|^2+C\tau\sum_{k=0}^{n-1}D^k. \tag{3.20}$$

Note that

$$\tau\sum_{k=0}^{n-1}\|R^k\|^2\le n\tau\max_{0\le k\le n-1}\|R^k\|^2\le T\,\mathcal{O}(\tau^2+h^2)^2 \tag{3.21}$$

and $D^0 \leq \mathcal{O}(\tau^2+h^2)^2$. It follows from (3.20) that

$$D^n \leq \mathcal{O}(\tau^2+h^2)^2 + T\,\mathcal{O}(\tau^2+h^2)^2 + C\tau\sum_{k=0}^{n-1} D^k.$$

i.e.

$$D^n \leq \mathcal{O}(\tau^2+h^2)^2 + C\tau\sum_{k=0}^{n-1} D^k. \tag{3.22}$$

According to Lemma 5, we have $D^n \leq \mathcal{O}(\tau^2+h^2)^2$. From the definition D^n, we have

$$\|e^n\| \leq \mathcal{O}(\tau^2+h^2), \qquad \|e^n_{xx}\| \leq \mathcal{O}(\tau^2+h^2).$$

From (3.17), we have $\|e^n_x\| \leq \mathcal{O}(\tau^2+h^2)$. It follows from Lemma 3 that

$$\|e^n\|_\infty \leq \mathcal{O}(\tau^2+h^2).$$

This completes the proof. □

Using a similar proof for Theorem 3.3, we can prove the following theorem.

Theorem 3.7 *Under the conditions of Theorem* 3.3*, the solution* u^n *of the difference scheme (2.6)–(2.9) is stable by the norm* $\|\cdot\|_\infty$.

4. Numerical results

In this section, some numerical tests are presented to verify the expected rate of convergence, utility, adaptability, and conservation property of the proposed scheme (2.6)-(2.9). The proposed method is applied for different values of p. The accuracy of the method is measured by using the norms

$$L_\infty = \max_{0\leq j\leq J}\left|u(x_j,t_n)-u_j^n\right|, \qquad L_2 = \sqrt{h\sum_{j=0}^{J}\left|u(x_j,t_n)-u_j^n\right|^2} \tag{4.1}$$

and order of the convergence is calculated by the formula

$$\text{order} = \frac{\log\left(L(\Delta_1)/L(\Delta_2)\right)}{\log 2} \tag{4.2}$$

where L is either L_∞ or L_2 error computed at the step size $\Delta_1 = h, \Delta_2 = h/2$ or $\Delta_1 = \tau, \Delta_2 = \tau/2$.

We consider the Rosenau–KdV–RLW equation (2.1)–(2.3) with the power law nonlinearity p and $\beta = 1$, $\gamma = 1$, $\alpha = 1$. The exact solution of the equations is given by [29]

$$u(x,t) = A\,\operatorname{sech}^{\frac{4}{p-1}}(B(x-vt)) \tag{4.3}$$

where

$$\begin{aligned} A &= \left[\left(\frac{\left(D-(p^2+2p+5)\right)^2}{-8(p+1)\beta\gamma+(p^2+2p+5)\left(D-(p^2+2p+5)\right)}\right)\left(\frac{(p+3)(3p+1)}{16(p+1)\alpha}\right)\right]^{\frac{1}{p-1}} \\ B &= \frac{p-1}{p+1}\sqrt{\frac{D-(p^2+2p+5)}{32\beta}} \\ D &= \sqrt{(p^2+2p+5)^2+16(p+1)^2\beta(\beta+\gamma)} \\ v &= \frac{\beta(p-1)^2}{4B^2(p^2+2p+5)-(p-1)^2\gamma}. \end{aligned}$$

The initial condition

$$u(x,0) = A\ \mathrm{sech}^{\frac{4}{p-1}}(Bx)$$

is obtained from the exact solution (4.3) by setting $t=0$.

Table 1. Rosenau–KdV–RLW equation (2.1) with $p=5$. Impact of the parameter θ with $h=0.1$, $\tau=0.01$, for $-40\le x\le 40$ at $T=5$.

θ	-1	$-1/2$	$-1/6$	0	$1/6$	$1/2$	1
$L_\infty\times 10^2$	3.26	1.89	1.02	0.60	0.34	0.61	1.76
$L_2\times 10^2$	6.42	3.86	2.26	1.50	0.83	1.09	3.17

Table 1 represents the impact of the parameter θ for various values in the range $[-1,1]$, on the error of the numerical scheme (2.6). We see that numerical approximation depends on the parameter θ. The minimum error is achieved for the value of $\theta=1/6$. We have carried out similar experiment for other values of p. In all experiments, we see that the choice of $\theta=1/(p+1)$ yields the minimum error.

In Table 2, we present some results for some particular choice of parameter θ. We note that the observed convergence rates agree well with the expected rate of convergence with respect to the L_∞ and L_2 error norms. In addition, when we use smaller space and time steps, we get smaller errors.

The errors in the sense of L_∞ norm and L_2 norm of the numerical solutions are listed in Tables 3 and 4 for $p=5$ and $p=8$, respectively. Numerical solutions for different values of h and k verify that the scheme (2.6) demonstrates the expected second-order convergence in both time and space directions. The log–log scale graph of the order of convergence for $p=5$ is depicted in Figure 1.

Figure 2 shows the solitary wave solutions for different power law nonlinearity p. From the figures it is obvious that the height of the solitary waves at different times is identical. This verifies the conservation of energy by the proposed scheme (2.6). We also list the conservation of the invariant (2.14) at different times in Table 5. It is clear that the invariant $E(0)$ remains constant during simulation

In order to investigate the sensitivity of the solitary wave propagation with respect to the third order dispersion coefficient β, we have performed a test for particular values of β. The following parameters are used in this test:

$$\gamma=\alpha=1, p=3, \theta=1/4, -40\le x\le 100, h=0.5,\ \tau=0.1$$

Figure 3 shows the amplitude of the wave for different value of β. From the figure, it is clear that for small values of β, the peak of the wave remains constant and we conclude that the soliton is stable. However, when

Table 2. Rosenau–KdV–RLW equation (2.1) with $p = 3$ for $-40 \le x \le 40$. Error estimated in the sense of L_∞ and L_2 at $T = 10$.

$\tau = h$	L_∞	$\frac{\|e(h,\tau)\|_\infty}{4\|e(h/2,\tau/2)\|_\infty}$	L_2	$\frac{\|e(h,\tau)\|_2}{4\|e(h/2,\tau/2)\|_2}$
$\theta = 0$				
0.5	2.757447×10^{0}	—	5.866344×10^{0}	—
0.25	6.138309×10^{-1}	1.123	1.3969681×10^{0}	1.050
0.125	2.455592×10^{-1}	0.625	5.674822×10^{-1}	0.615
0.0625	1.118155×10^{-1}	0.549	2.603788×10^{-1}	0.545
$\theta = 1/4$				
0.5	2.093416×10^{-1}	—	5.633075×10^{-1}	—
0.25	1.053109×10^{-1}	0.497	2.900051×10^{-1}	0.485
0.125	5.268842×10^{-2}	0.499	1.481474×10^{-1}	0.489
0.0625	2.639791×10^{-2}	0.498	7.502810×10^{-2}	0.493
$\theta = 1/2$				
0.5	4.401416×10^{-1}	—	9.319403×10^{-1}	—
0.25	2.781047×10^{-1}	0.395	5.747320×10^{-1}	0.405
0.125	1.569375×10^{-1}	0.443	3.197992×10^{-1}	0.449
0.0625	8.325497×10^{-2}	0.471	1.685063×10^{-1}	0.474
$\theta = 3/4$				
0.5	5.928871×10^{-1}	—	1.236796×10^{0}	—
0.25	4.322233×10^{-1}	0.343	8.876284×10^{-1}	0.348
0.125	2.744779×10^{-1}	0.393	5.575084×10^{-1}	0.398
0.0625	1.575200×10^{-1}	0.435	3.177538×10^{-1}	0.438
$\theta = 1$				
0.5	6.771554×10^{-1}	—	1.419035×10^{0}	—
0.25	5.308451×10^{-1}	0.319	1.101512×10^{0}	0.3220
0.125	3.635146×10^{-1}	0.365	7.459152×10^{-1}	0.369
0.0625	2.208605×10^{-1}	0.411	4.498644×10^{-1}	0.414

Table 3. Rosenau-KdV-RLW equation (2.1) with $p = 5$ and $\theta = 1/6$, for $-40 \le x \le 40$. Error estimated in the sense of L_∞ and L_2 at $T = 10$

$\tau = h$	L_∞	$\frac{\|e(h,\tau)\|_\infty}{4\|e(h/2,\tau/2)\|_\infty}$	L_2	$\frac{\|e(h,\tau)\|_2}{4\|e(h/2,\tau/2)\|_2}$
0.5	1.960892×10^{-1}	—	4.931433×10^{-1}	—
0.25	1.048603×10^{-1}	0.467	2.802211×10^{-1}	0.440
0.125	5.405413×10^{-2}	0.485	1.476313×10^{-1}	0.474
0.0625	2.739923×10^{-2}	0.493	7.541186×10^{-2}	0.489

β is increased, the soliton amplitude decreases dramatically, and the soliton eventually collapses due to the dispersion radiation. Figure 4 shows this phenomenon.

Table 6 represents the numerical results in terms of L_∞ norm obtained by the scheme [37] by using $p = 2$, $\alpha = 0.5$, $\beta = \gamma = 1$ on the spatial domain $[-40, 40]$ at time $T = 10$. We see that there is good agreement with the numerical results presented in [37].

Table 4. Rosenau-KdV-RLW equation (2.1) with $p = 8$ and $\theta = 1/9$, for $-40 \le x \le 40$. Error estimated in the sense of L_∞ and L_2 at $T = 10$.

$\tau = h$	L_∞	$\frac{\|e(h,\tau)\|_\infty}{4\|e(h/2,\tau/2)\|_\infty}$	L_2	$\frac{\|e(h,\tau)\|_2}{4\|e(h/2,\tau/2)\|_2}$
0.5	2.556694×10^{-1}	—	6.353800×10^{-1}	—
0.25	1.302380×10^{-1}	0.491	3.324394×10^{-1}	0.478
0.125	6.346584×10^{-2}	0.513	1.643340×10^{-1}	0.506
0.0625	3.117148×10^{-2}	0.509	8.130424×10^{-2}	0.505

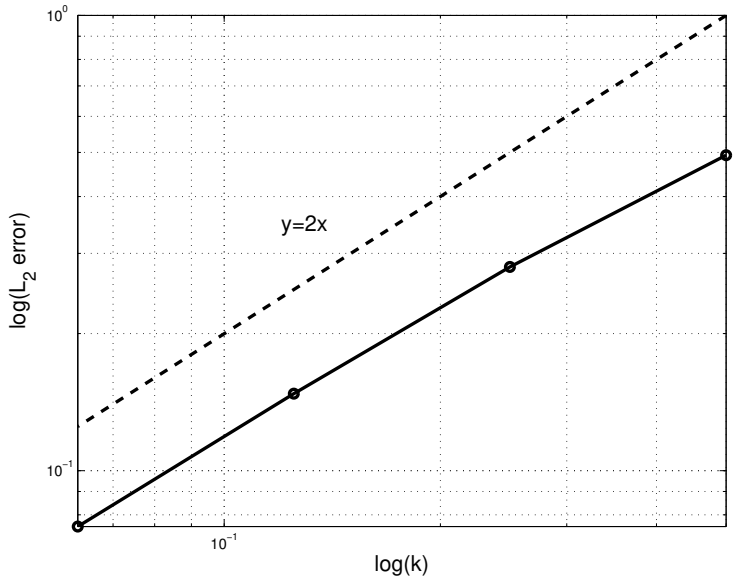

Figure 1. Log log scale graph of L_2 error versus time step for $p = 5$.

Table 5. Rosenau-KdV-RLW equation (2.1): Conservation of energy (2.14) on $-40 \le x \le 100$ with $h = 0.1$, $\tau = 0.01$.

(p, θ)	$(2, 1/3)$	$(3, 1/4)$	$(5, 1/6)$	$(8, 1/9)$
$E(0)$	10.9291784372	6.5365521351	5.1104564747	5.2430504512
$E(500)$	10.9291784378	6.5365521351	5.1104563445	5.2430504509
$E(1000)$	10.9291784374	6.5365521353	5.1104563445	5.2430504509

Table 6. Comparison of L_∞ norm.

	$\tau = h = 0.5$	$\tau = h = 0.25$	$\tau = h = 0.125$	$\tau = h = 0.0625$
Scheme (2.6), $p = 2$	2.07328×10^{0}	5.59377×10^{-1}	1.50129×10^{-1}	4.00242×10^{-2}
Scheme[37]	1.45901×10^{0}	3.72110×10^{-1}	9.34987×10^{-2}	2.34123×10^{-2}

4.1. Evolution of a Gaussian wave packet

The formation of a train of solitary wave from the breakup, dissolution, or decay of a single initial Gaussian shaped pulse has fascinated many researchers working on solution of nonlinear PDEs such as the KdV equation [3, 35, 39], RLW equation [10], and the generalized Rosenau [27] equation. In this section, Gaussian pulse is

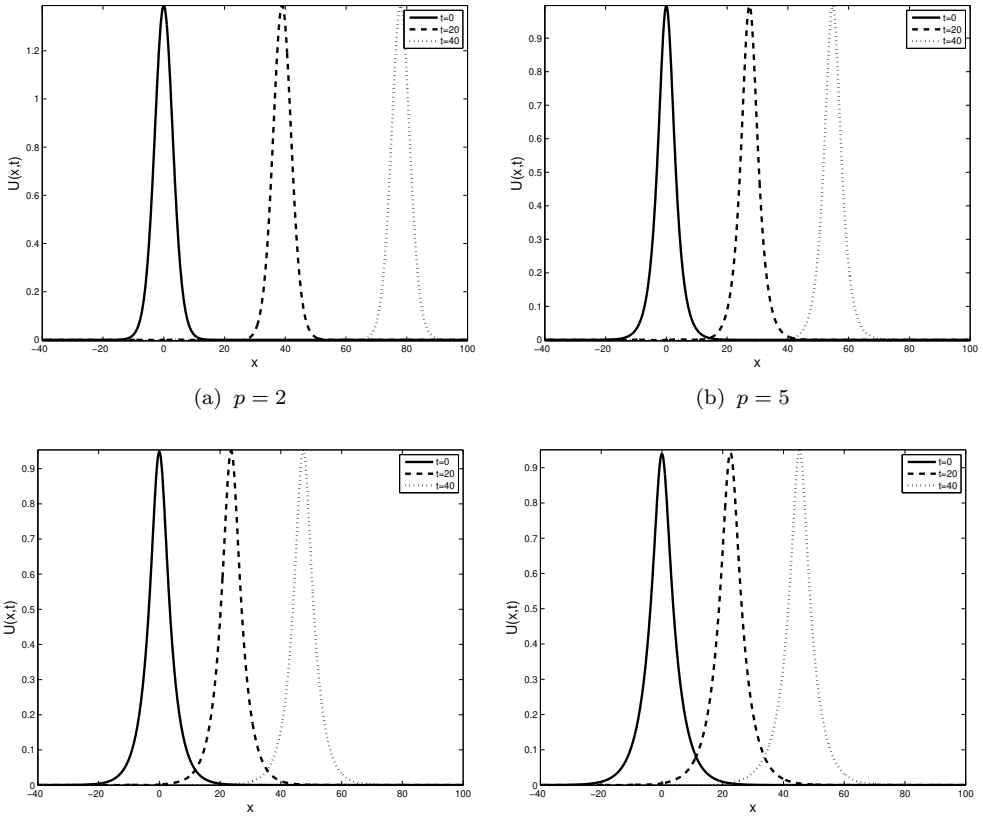

(a) $p = 2$ (b) $p = 5$

(c) $p = 8$ (d) $p = 10$

Figure 2. Solitary wave solutions with $h = 0.5,\ \tau = 0.01$.

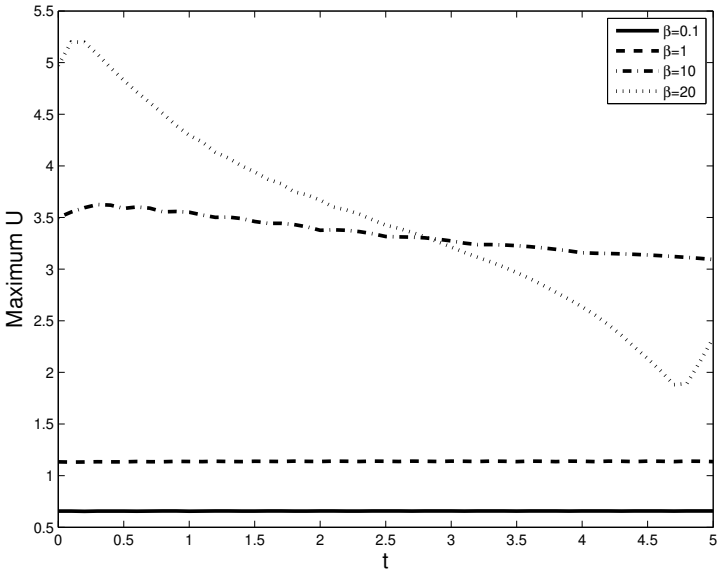

Figure 3. Dispersion effect for $p = 3$. Evolution of the maximum value for the amplitude of a pulse for several values of the dispersion coefficient β.

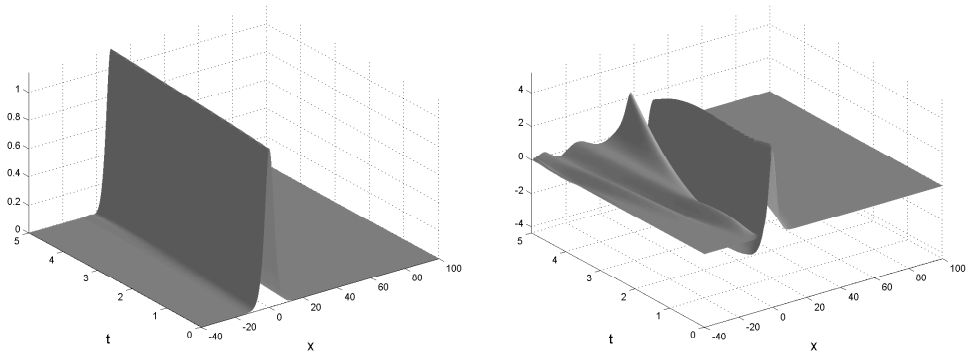

(a) $\beta = 1$ (b) $\beta = 20$

Figure 4. Influence of the dispersion coefficient β on the solitary wave evolution.

used to provide the initial condition to study the wave generation from the generalized Rosenau–KdV–RLW equation (2.1) by means of the conservative scheme (2.6).

We consider the generalized Rosenau–KdV–RLW equation (2.1) with $\beta = 1$ and $p = 2$ in the domain $(x,t) \in [-80, 150] \times [0, 70]$ with the Gaussian initial condition

$$u(x,0) = e^{-\frac{(x-20)^2}{100}}, \quad x_L \leq x \leq x_R \tag{4.4}$$

and the boundary conditions in (2.3) using $h = 0.2$ and $\tau = 0.05$. The equation (4.4) represents a pulse centered at the position $x_0 = -20$. This pulse is positive and has the unit amplitude.

First we choose $\alpha = 1$ and study the effect of the dispersive coefficient γ. Figure 5 represents how the solution $u(x,t)$ with $\gamma = 1/10$ looks like with the initial condition (4.4). From the figure, we see that the initial Gaussian pulse does not propagate to the right as a single solitary wave. Instead, it changes shapes, breaks into a train of solitary wave and propagates to the right by leaving behind a small oscillatory disturbance. The initial pulse has evolved into three separated solitary waves by the time $t = 70$ steepening the leading front. For $\gamma = 2$, the results presented in Figure 6 show that initial Gaussian profile generates two solitary waves with small radiations. This figure also shows that the amplitude of the wave decreases from leading pulse to the trailing pulse. Numerical results for $\gamma = 7$ is given in Figure 7. The initial Gaussian pulse evolves as a single traveling solitary wave moving to the right by leaving a small disturbance. A closer examination of the initial profile and the final profile indicates that the wave profile at $t = 70$ has an amplitude that is only 4.5% higher than unity for the initial Gaussian profile. In addition, wave width of both pulse are approximately the same. For these reasons, the solitary wave almost carries away the majority of the conservation laws such as mass and the energy.

Now, we choose $\gamma = 1$ and study the effect of the nonlinear advection coefficient α. Figures 8 and 9 illustrate the numerical solution of the Gaussian pulse evolution for $\alpha = 0.15$ and $\alpha = 0.5$ respectively. From Figure 8 we see that initial Gaussian profile propagates to the right as a solitary wave without splitting. Some small radiations are observed between the left boundary and the trailing wave. Additionally, the wave profile at $t = 70$ has an amplitude that is only 2.8% higher than unity for the initial Gaussian profile. The wave width of both pulse are approximately the same. Therefore, conservation laws such as mass and the energy of the equation are almost conserved throughout the evolution. Numerical results with $\alpha = 0.5$ are given in Figure 9. We see that when we increase the value of the nonlinear term α, the initial Gaussian profile evolves into two

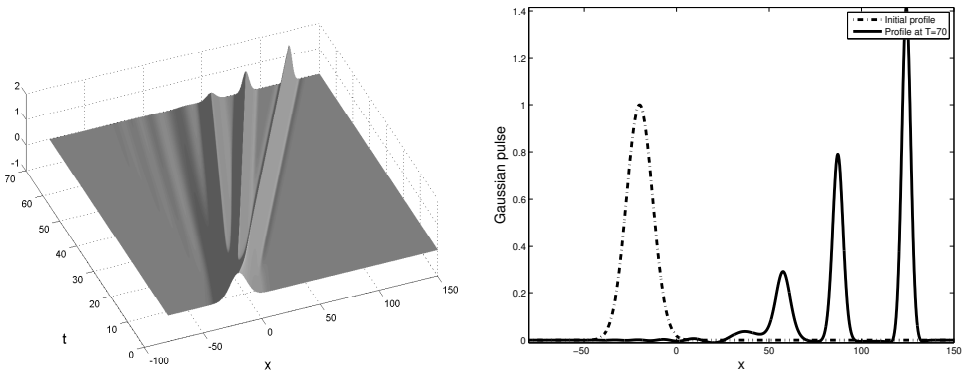

(a) Time evolution. (b) The profile at the time $T = 70$.

Figure 5. Solitary waves evolving from an initial Gaussian profile with $\alpha = 1$ and $\gamma = 1/10$.

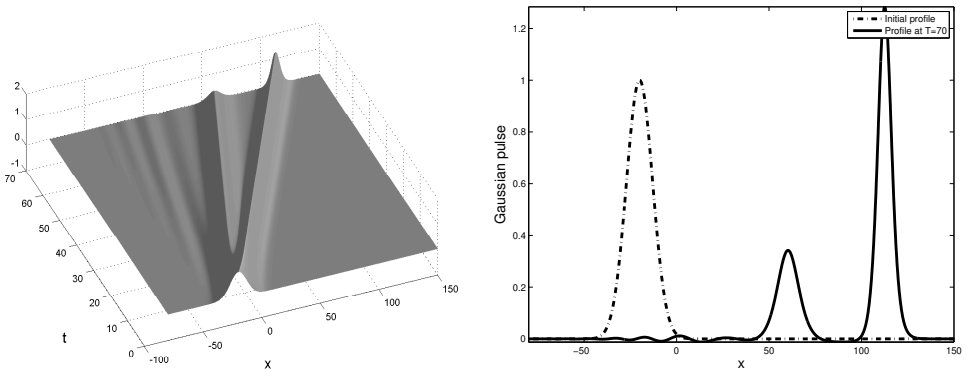

(a) Time evolution. (b) The profile at the time $T = 70$.

Figure 6. Solitary waves evolving from an initial Gaussian profile with $\alpha = 1$ and $\gamma = 2$.

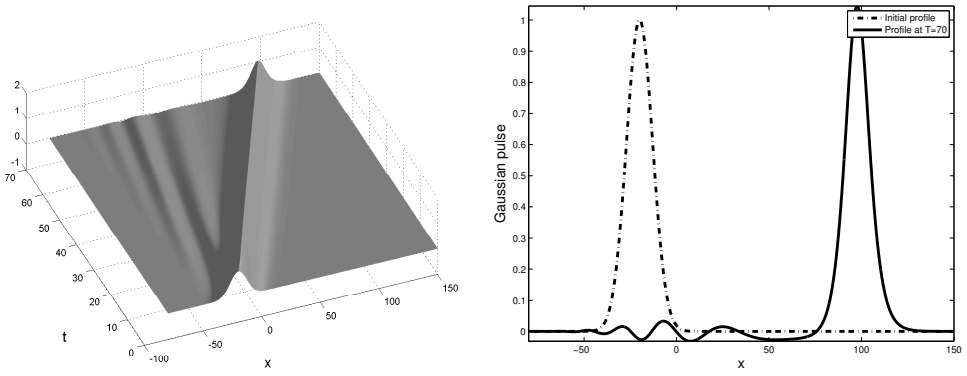

(a) Time evolution. (b) The profile at the time $T = 70$.

Figure 7. Solitary waves evolving from an initial Gaussian profile with $\alpha = 1$ and $\gamma = 7$.

separated solitary waves by the time $t = 70$. The figure also reveals that the amplitude of the leading wave increases.

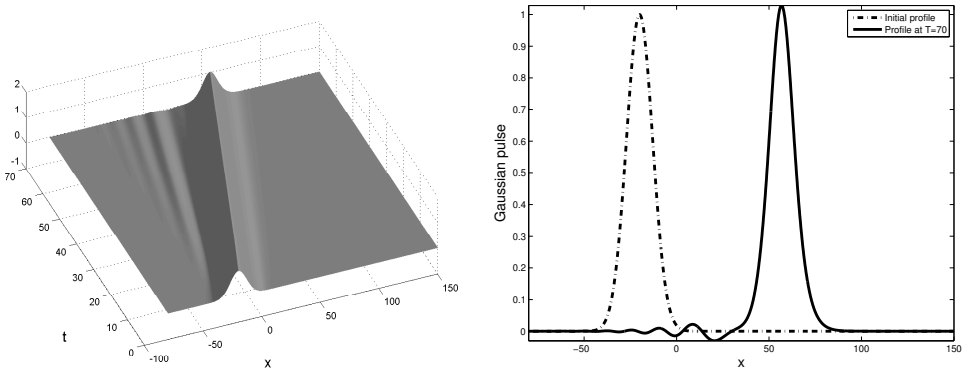

(a) Time evolution. (b) The profile at the time $T = 70$.

Figure 8. Solitary waves evolving from an initial Gaussian profile with $\alpha = 0.15$ and $\gamma = 1$.

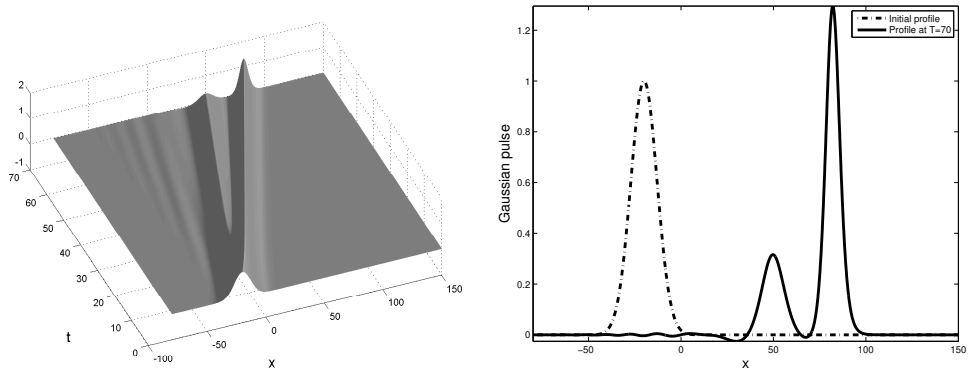

(a) Time evolution. (b) The profile at the time $T = 70$.

Figure 9. Solitary waves evolving from an initial Gaussian profile with $\alpha = 0.5$ and $\gamma = 1$.

5. Conclusions

We proposed a two-level and linear scheme for the numerical solution of the generalized Rosenau–KdV–RLW equation. Some prior estimations of the difference scheme are proved. It showed that the proposed scheme is conservative. Existence, uniqueness, convergence, and stability with $\mathcal{O}(\tau^2 + h^2)$ in the maximum-norm of the difference scheme are analyzed. Numerical results confirm the theoretical results that the proposed scheme is conservative and second–order convergent. Moreover, the proposed scheme simulates the solitary wave solution of the generalized Rosenau–KdV–RLW equation very well in long time without showing any instability. The formation of a train of solitary wave from the generalized Rosenau–KdV–RLW equation subject to the Gaussian initial condition is also studied in terms of the dispersion coefficient and nonlinear coefficients of the equation. It is observed that a singe Gaussian pulse breaks into train of rightward traveling solitary waves when the values of the dispersion coefficient and nonlinear coefficient are changed. It is also found that the initial Gaussian pulse changes shape slightly and propagates rightward as a single solitary wave and leaves behind a small oscillatory disturbance. We remark that no instability has been detected from our numerical tests.

References

[1] Achouri T, Khiari N, Omrani K. On the convergence of the difference schemes for the Benjiamin-Bona-Mahony (BBM) equation. Applied Mathematics and Computation 2006; 182 : 999-1005.

[2] Atouani N, Omrani K. Galerkin finite element method for the Rosenau-RLW equation, Computers and Mathematics with Applications 2013; 66 (33): 289-303.

[3] Berezin Y, Karpman VI. Nonlinear evolution of disturbances in plasmas and other dispersive media. Soviet Physics JETP 1967; 24: 1049-1056.

[4] Bildik N, Deniz S. Solving the burgers's and regularized long wave equations using the new perturbation iteration technique. Numerical Methods for Partial Differential Equations 2018; 34 (5): 1489-1501.

[5] Bildik N, Deniz S. New analytic approximate solutions to the generalized regularized long wave equations. Bulletin of the Korean Mathematical Society, 2018; 55 (3): 749-762.

[6] Boussinesq J. Essai sur la theorie des eaux courantes. Memoires presentes par divers savants a l'Academie des Sciences de l'Institut National de France XXIII 1877: 1-680 (in French).

[7] Demiray H. Higher order approximations in reductive perturbation methods: strongly dispersive waves. Communications in Nonlinear Science and Numerical Simulation 2005; 10 (5): 549-558.

[8] Dogan A. Numerical solution of regularized long wave equation using Petrov–Galerkin method. Communications in Numerical Methods in Engineering 2001; 17: 485-494.

[9] Esfahani A. Solitary wave solutions for generalized Rosenau- KdV equation. Communications in Theoretical Physics 2011; 55 (3): 396-398

[10] Gardner LRT, Gardner GA, Ayoub A, Amein NK. Simulations of the EW undular bore. Communications in Numerical Methods in Engineering 1997; 13: 583-592

[11] Hu J, Xu Y, Hu B. Conservative linear difference scheme for Rosenau-KdV equation. Advances in Mathematical Physics 2013; 423718.

[12] Khalifa A, Raslan K, Alzubaidi H. A collocation method with cubic B-spline for solving the MRLW eqution. Journal of Computational and Applied Mathematics 2008; 212: 406-418.

[13] Korteweg DJ, deVries G. On the change of form of long waves advancing in a rectangular canal, and on a new type of long stationary waves. Philosophical Magazine and Journal of Science 1895; 39 (5): 422-443. doi:10.1080/14786449508620739

[14] Labidi M, Omrani K. Numerical simulation of the modified regularized long wave equation by He's variational iteration method. Numerical Methods Partial Differential Equation 2011; 27: 478-489.

[15] Lakestani M. Numerical solutions of the KdV equation using B-spline functions. Iranian Journal of Science and Technology, Transaction A: Science 2017; 41 (2): 409-417.

[16] Luo Y, Xu Y, Feng M. Conservative difference scheme for generalized Rosenau-KdV equation. Advances in Mathematical Physics 2014; 986098.

[17] Manafian J, Lakestani M, Bekir A. Study of the analytical treatment of the $(2+1)$-dimensional zoomeron, the duffing and the SRLW equations via a new analytical approach. International Journal of Applied and Computational Mathematics 2016; 2 (2): 243-268.

[18] Manafian J, Lakestani M. Solitary wave and periodic wave solutions for Burgers, Fisher, Huxley and combined forms of these equations by the (G'/G)-expansion method. Pramana Journal of Physics 2015; 85 (1): 31-52

[19] Mittal RC, Jain RK. Numerical solution of general Rosenau- RLW equation using quintic B-Splines collocation method. Communication in Numerical Analysis 2012; 00129.

[20] Neirameh A, Memarian N. New analytical soliton type solutions for double layers structure model of extended KdV equation. Computational Methods for Differential Equations 2017; 5 (4): 256-270.

[21] Pan X, Zhang L. On the convergence of a conservative numerical scheme for the usual Rosenau-RLW equation. Applied Mathematical Modellling 2012; 36: 3371-3378.

[22] Pan X, Zhang L. Numerical simulation for general Rosenau- RLW equation: An average linearized conservative scheme. Mathematical Problems in Engineering 2012; 517818.

[23] Pan X, Zhang L. On the convergence of a conservative numerical scheme for the usual Rosenau–RLW equation. Applied Mathematical Modelling 2012; 36: 3371-3378.

[24] Pan X, Zheng K, Zhang L. Finite difference discretization of the Rosenau-RLW equation. Applicable Analysis 2013; 92 (12): 2578-2589.

[25] Pan X, Wang Y, Zhang L. Numerical analysis of a pseudo-compact C–N conservative scheme for the Rosenau–KdV equation coupling with the Rosenau–RLW equation. Boundary Value Problems 2015; 65. doi:10.1186/s13661-015-0328-2

[26] Peregrine DH. Calculations of the development of an unduiar bore. Journal of Fluid Mechanics 1966; 25: 321-330.

[27] Ramos JI, Garcia-Lopez CM. Solitary wave formation from a generalized Rosenau equation. Mathematical Problems in Engineering 2016; 4618364.

[28] Razborova P, Triki H, Biswas A. Perturbation of dispersive shallow water waves. Ocean Engineering 2013; 63: 1-7.

[29] Razborava P, Ahmed B, Biswas A. Soliton, Shock Waves and conservation Laws of Rosenau-kdv-RLW Equation with power law Nonlinearity. Applied Mathematics and Information Science 2014; 8 (2): 485-491.

[30] Razborova P, Moraru L, Biswas A. Perturbation of dispersive shallow water waves with Rosenau-KdV-RLW equation and power law nonlinearity. Romanian Journal of Physics 2014; 59 (7-8): 658-676.

[31] Rosenau P. A quasi-continuous description of a nonlinear transmissi on line. Physica Scripta 1986; 34: 827-829.

[32] Rosenau P. Dynamics of dense discrete systems. Progress of Theoretical Physics 1988; 79: 1028-1042.

[33] Roshid H. Multi-soliton of the (2+1)-dimensional Calogero-Bogoyavlenskii-Schiff equation and KdV equation. Computational Methods for Differential Equations 2019; 7 (1): 86-95.

[34] Saha A. Topological 1–soliton solutions for the generalized Rosenau-KdV equation. Fundamental Journal of Mathematical Physics 2012; 2 (1): 19-23.

[35] Shen J. A new dual-Petrov–Galerkin method for third and higher odd-order differential equations: application to the KdV equation. SIAM Journal of Numerical Analysis 2003; 41 (5): 1595-1619.

[36] Wang X, Dai W. A three-level linear implicit conservative scheme for the Rosenau-KdV-RLW equation. Journal of Computational and Applied Mathematics 2018; 330: 295-306.

[37] Wongsaijai B, Poochinapan K. A tree-level average implicit finite difference scheme to solve equation obtained by coupling the Rosenau-KdV equation and the Rosenau-RLW equation. Applied Mathematics and Computation 2014; 245: 289-304.

[38] Zhang Q, Gao F. A fully-discrete local discontinuous Galerkin method for convection-dominated Sobolev equation. Journal of Scientific Computation 2012; 51: 107-134.

[39] Zheng C. Numerical simulation of a modified KdV equation on the whole real axis. Numerical Mathematics 2006; 105: 315-335.

[40] Zhou YL. Application of Discrete Functional Analysis to the Finite Difference Methods. Beijing, China: International Academic Publishers, 1990.

[41] Zuo JM. Solitons and periodic solutions for the Rosenau- KdV and Rosenau-Kawahara equations. Applied Mathematics and Computation 2009; 215 (2): 835-840.

[42] Zuo JM, Zhang YM, Zhang TD. A new conservative difference scheme for the general Rosenau-RLW equation. Boundary Value Problem 2010; 516260.